5441

LIBRARY USE ONLY

NUWC-NPT Technical Memorandum 990017

Copy 1

Naval Undersea Warfare Center Division
Newport, Rhode Island

MODIFIED AMPLITUDE AND STROUHAL NUMBER SCALING FOR CORRECTION OF TURBULENT WALL PRESSURE FLUCTUATIONS

Thomas A. Galib
Torpedo Systems Department

22 February 1999

Approved for public release; distribution is unlimited.

LIBRARY USE ONLY

Report Documentation Page

Form Approved
OMB No. 0704-0188

Public reporting burden for the collection of information is estimated to average 1 hour per response, including the time for reviewing instructions, searching existing data sources, gathering and maintaining the data needed, and completing and reviewing the collection of information. Send comments regarding this burden estimate or any other aspect of this collection of information, including suggestions for reducing this burden, to Washington Headquarters Services, Directorate for Information Operations and Reports, 1215 Jefferson Davis Highway, Suite 1204, Arlington VA 22202-4302. Respondents should be aware that notwithstanding any other provision of law, no person shall be subject to a penalty for failing to comply with a collection of information if it does not display a currently valid OMB control number.

1. REPORT DATE	2. REPORT TYPE	3. DATES COVERED
22 FEB 1999	**Technical Memo**	**22-02-1999 to 22-02-1999**

4. TITLE AND SUBTITLE
Modified Amplitude and Strouhal Number Scaling for Correction of Turbulent Wall Pressure Fluctuations

5a. CONTRACT NUMBER
5b. GRANT NUMBER
5c. PROGRAM ELEMENT NUMBER

6. AUTHOR(S)
Thomas Galib

5d. PROJECT NUMBER
5e. TASK NUMBER
5f. WORK UNIT NUMBER

7. PERFORMING ORGANIZATION NAME(S) AND ADDRESS(ES)
Naval Undersea Warfare Center Division,1176 Howell Street,Newport,RI,02841

8. PERFORMING ORGANIZATION REPORT NUMBER
TM 990017

9. SPONSORING/MONITORING AGENCY NAME(S) AND ADDRESS(ES)

10. SPONSOR/MONITOR'S ACRONYM(S)
SEA 92R

11. SPONSOR/MONITOR'S REPORT NUMBER(S)

12. DISTRIBUTION/AVAILABILITY STATEMENT
Approved for public release; distribution unlimited

13. SUPPLEMENTARY NOTES
NUWC2015

14. ABSTRACT
Pressure fluctuations were measured in an external turbulent boundary layer over a buoyantly propelled axisymmetric body of revolution. Data were measured for three cases: 69.7 feet/second in fresh water, 43.2 feet/second in fresh water, and 70.9 feet/second in salt water. The fresh water temperature was 39??F and the salt water temperature was 70??F, resulting in axial length Reynolds numbers of 6.88x10^6, 4.27x10^6, and 3.21x10^6 at the measurement locations. The fresh water measurements were made in a fully developed turbulent boundary layer, following natural transition, with a near zero (very mildly adverse) pressure gradient. The salt water measurements were made in a favorable pressure gradient following a flow trip to force transition. The momentum thickness Reynolds number Re^8 was greater than 4400 for all measurements, and the data were scaled with outer variables.

15. SUBJECT TERMS
pressure fluctuations; Reynolds number; turbulent boundary layer; Corcos correction factors; Strouhal

16. SECURITY CLASSIFICATION OF:			17. LIMITATION OF ABSTRACT	18. NUMBER OF PAGES	19a. NAME OF RESPONSIBLE PERSON
a. REPORT	b. ABSTRACT	c. THIS PAGE			
unclassified	**unclassified**	**unclassified**	**Same as Report (SAR)**	**23**	

ABSTRACT

Pressure fluctuations were measured in an external turbulent boundary layer over a buoyantly propelled axisymmetric body of revolution. Data were measured for three cases: 69.7 feet/second in fresh water, 43.2 feet/second in fresh water, and 70.9 feet/second in salt water. The fresh water temperature was 39°F and the salt water temperaure was 70°F, resulting in axial length Reynolds numbers of 6.88×10^6, 4.27×10^6, and 3.21×10^6 at the measurement locations. The fresh water measurements were made in a fully developed turbulent boundary layer, following natural transition, with a near zero (very mildly adverse) pressure gradient. The salt water measurements were made in a favorable pressure gradient following a flow trip to force transition. The momentum thickness Reynolds number Re_θ was greater than 4400 for all measurements, and the data were scaled with outer variables.

The turbulence data were corrected using Corcos correction factors and then further scaled in both amplitude and frequency by $\left(r/\delta^*\right)^{1/2}$, in an attempt to resolve spatial resolution effects. This resulted in excellent agreement among the spectra to a modified Strouhal number of $\left(\frac{\omega\delta^*}{U_\infty}\right)\left(r/\delta^*\right)^{1/2}=1$, which was the range of validity for the data. A second data set, in which all of the measurements were from one run, was also considered. In this case (constant freestream velocity and increasing displacement thickness with downstream measurement location), differences in spatial resolution effects were resolved with the modified Strouhal number as above, but the amplitude scaled somewhat better with r/δ^*.

ADMINISTRATIVE INFORMATION

This investigation was done as part of the Advanced Hydrodynamic Sail program. The sponsoring activity was SEA 92R (D. Dozier). The NUWC program manager was George McNamara.

ACKNOWLEDGMENTS

Appreciation is extended to all who were invoved in the 1990 and 1991 BTV experiments, including NUWC and United Kingdom/ Admiralty Research Establishment personnel.

TABLE OF CONTENTS

LIST OF ILLUSTRATIONS

INTRODUCTION

Scaling of turbulent pressure fluctuation spectra has been of interest to hydrodynamicists since the turbulence corrections proposed by Corcos (reference 1) 35 years ago. Use of amplitude and frequency correction factors allows comparison of investigations having different fluid media, transducer sizes, boundary layer displacement and momentum thicknesses, and freestream velocities.

For the purposes of this investigation, outer variables $\frac{\phi(\omega)}{\rho^2 U_\infty{}^3 \delta^*}$ vs $\frac{\omega\delta^*}{U_\infty}$ were used for nondimensionalizing the spectra. In these variables, $\phi(\omega)$ is the Corcos corrected pressure, ρ is the fluid density, U_∞ is the freestream velocity, δ^* is the displacement thickness, and ω is the frequency in radians per second. The momentum thickness Reynolds number Re_θ was greater than 4400 for all data. An excellent comparison of several investigations is given by Keith et al. (reference 2). One of the conclusions of Keith's investigation is that outer variable scaling is effective for momentum thickness Reynolds numbers greater than 4500. Another conclusion from Keith's investigation is that spatial resolution of the transducer is very important for measuring and comparing turbulence spectra. This is in full agreement with a previous investigation by Galib and Zadina (reference 3), in which finite size piezoelectric sensor measurements were compared with "point" piezoresistive measurements in a turbulent boundary layer. There is an excellent discussion in the paper by Keith et al. concerning how comparisons of turbulence data can depend on the experimental method because of attenuations at a given Strouhal frequency $\frac{\omega\delta^*}{U_\infty}$. This is due to the turbulence measurement attenuation, which is dependent upon the ratio of transducer radius to the displacement thickness r/δ^*. For example, within a given experiment with constant freestream velocity, a row of sensors of radius r will yield a downstream reduction of r/δ^* (increased resolution) due to a growing displacement thickness. For a sensor in a given location, however, an increase in flow velocity will result in an increase of r/δ^* (decreased resolution) at the measurement location, due to a reduction in displacement thickness. Both of these cases are considered in this investigation. A full discussion of transducer response to turbulent pressure fluctuations can be found in Corcos and will not be repeated here except to emphasize that the transducer response is a function of $\omega r/U_c$ and of r/δ^*, where ω is the frequency in radians per second, r is the transducer radius, U_c is the convective velocity (assumed to be 0.7 of the freestream velocity for this experiment), and δ^* is the displacement thickness. The investigation reported on herein

is an attempt to quantify the response dependence on r/δ^*, while using Corcos corrections for $\omega r/U_c$.

In terms of the convective wavenumber k_c, the effect of multiplying $\frac{\omega\delta^*}{U_\infty}$ by $\left(r/\delta^*\right)^{1/2}$ is as follows:

$$\left(\frac{\omega\delta^*}{U_\infty}\right)\left(r/\delta^*\right)^{1/2}=\frac{\omega}{U_\infty}\left(r\delta^*\right)^{1/2}=\frac{\omega}{U_c}\frac{U_c}{U_\infty}\left(r\delta^*\right)^{1/2}=\frac{U_c}{U_\infty}[k_c\left(r\delta^*\right)^{1/2}]$$
$$=\frac{U_c}{U_\infty}k_c r\left(\delta^*/r\right)^{1/2}.$$

The first term in the last line of this expression is related to the size of the pressure fluctuations that will be measured; i.e., larger pressure fluctuations in the outer part of the boundary layer are convected at higher velocities. The other two terms are related to the ability of the sensor to measure the turbulence; i.e., a transducer that is large compared to the size of fluctuations in the boundary layer will attenuate the higher frequency measurements. Note that the term $k_c r$ is equivalent to $\omega r/U_c$, which is the important parameter for Corcos corrections of transducer response.

EXPERIMENT

Experiments were conducted both in a deep fresh water lake (Lake Pend Oreille) at a facility operated by the Naval Surface Warfare Center/ Acoustic Research Detachment in Bayview, Idaho, and in the ocean at the Atlantic Undersea Test and Evaluation Center in the Bahamas. The same buoyant test vehicle was used for both the lake and ocean experiments. The test vehicle was propelled vertically from a depth of 1100 feet by its buoyancy (figure 1).

The buoyant test vehicle was a 21-inch-diameter axisymmetric body approximately 27 feet in length. The vehicle included a weight section which held a symmetrically distributed array of cylindrical lead weights. Depending upon the amount of weight in this section, vehicle speeds of 40 to 75 feet/second were attainable. The range for these experiments was 43 to 71 feet/second.

The nose of the test vehicle was instrumented with piezoelectric pressure transducers to measure the pressure fluctuations associated with the developing boundary layer and the resulting turbulence. The transducers were PCB model 112M149 having a sensitivity of 50 mV/psi (-26 dB//1 V/psi). The physical diameter of the transducers was 0.218 inch, and the effective diameter, based on -6dB sensitivity, was determined to be

0.12 inch (reference 3). The pressure transducers were mounted in a carbon-graphite nose shell, with stainless steel inserts, as shown in figure 2. The entire shell surface was covered with a 0.125-inch elastomer to provide a smooth surface for the boundary layer. Thus, in this configuration, the transducers did not interfere with the flow over the nose surface.

At Lake Pend Oreille, the vehicle was hauled down to a depth of 1100 feet via a cable attached to an onshore winch. Once the vehicle was stopped at the bottom of the lake, the onboard Honeywell 5600C tape recorder was powered, and ambient data from all sensors were recorded for 30 seconds. Following the ambient recording, the vehicle released itself from the cable and buoyantly ascended toward the surface. For a vehicle speed of 70 feet/second, steady-state conditions were achieved at a depth of 700 feet. At a depth of 160 feet, the fins kicked over, turning the vehicle so that it would not broach the surface. The data reported on herein were recorded during the steady-state portion of the run, which for the higher speed, was a 5-second interval between 550 and 200 feet; for the lower speed, data were measured between 415 and 200 feet. The ocean operation was identical, except that the winch was located on a barge near the test range.

DATA ANALYSIS

Pressure fluctuation data from the onboard analog tape recorder were low-pass filtered at 5 kHz, which is beyond the range of useful turbulence measurements for these experiments (reference 4), and digitized at a frequency of 12.5 kHz. All 70 feet/second data had at least 6 dB signal to noise up to 3 kHz; 45 feet/second data were good to 1.8 kHz; and these are therefore the frequency ranges of data upon which the conclusions are based. Spectral analysis was performed on an HP 3561 spectrum analyzer with 35 averages and a Hanning window, resulting in a bandwidth of 18.75 Hz, which was later subtracted from the spectra. Dimensional spectra are presented to 5 kHz, however, to show spectral trends when turbulence is no longer measured due to the spatial averaging considerations discussed above, and are instead contaminated by vibration (reference 4). Nondimensional spectra were plotted (only in the frequency ranges containing uncontaminated turbulence data) in outer variables, both uncorrected and with Corcos corrections, and were then scaled for both cases by $\left(r/\delta^*\right)^{1/2}$. The effective transducer radius, as determined in reference 3, was used for data analysis. In the uncorrected case, the term $\phi(\omega)$ is just the measured pressure. The displacement thicknesses of the turbulent boundary layer at the measurement locations were computed by the Transition Analysis Program System (reference 5). Although the uncorrected data were analyzed, they are not shown herein, because the Corcos corrections were necessary to collapse the spectra.

RESULTS

As mentioned previously in this report, two cases were considered for analysis of the turbulent boundary layer pressure fluctuations. In the first case, measurements among several runs were compared, so that freestream velocity and other flow parameters were varied. In the second case, measurements from several locations taken simultaneously from one run were compared. For all of the data shown in this report, the transducers were the same size.

Results are shown for three representative transducers (see table 1 below) for the first case.

Table 1: Pressure Transducers and Flow Parameters for Varying Freestream Velocity

Transducer _Run	Velocity (ft/second)	Pressure Gradient	Re_x	Re_{δ^*}	Re_θ	r/δ^*
B7_1521	69.7	adverse $\cong 0$	6.88×10^6	8.86×10^3	6.55×10^3	2.28
A8_1522	43.2	adverse $\cong 0$	4.27×10^6	6.13×10^3	4.50×10^3	2.04
A1_1588	70.9	favorable	3.21×10^6	5.92×10^3	4.44×10^3	5.33

The locations of the transducers considered in table 1 are shown in figure 3. The spectra of pressure fluctuations measured by the three transducers are shown in figure 4. Evident from figure 4 is the spread in the frequency content of the data, as well as amplitude differences. These measured spectra were corrected using the Corcos method and plotted with outer variables, as shown in figure 5. The more rapid high frequency rolloff in the spectrum for A1_1588 is due to the much higher value of r/δ^*. In addition, it is evident that the rolloff begins at a lower nondimensional frequency (Strouhal number), compared with the other two spectra in figure 5. This is in contrast to the measured spectra of figure 4. The Corcos corrected data of figure 5 were further corrected in frequency by a factor of $\left(r/\delta^*\right)^{1/2}$, the results of which are shown in figure 6. Notice that the rolloff characteristics of the three spectra are now identical; i.e., they begin at the same modified Strouhal number (equal to 0.3) and attenuate with the same slope. However, differences in the amplitudes still remain. The amplitude differences were resolved by employing an amplitude scale factor of $\left(r/\delta^*\right)^{1/2}$, as shown in figure 7.

The second case considered in this study consisted of maintaining constant flow velocity, with increasing displacement thickness for downstream measurement locations. Important flow parameters are shown in table 2.

Table 2: Pressure Transducers and Flow Parameters for Constant Freestream Velocity

Transducer _Run	Velocity (ft/second)	Pressure Gradient	Re_x	Re_{δ^*}	Re_θ	r/δ^*
A1_1588	70.9	favorable	3.21×10^6	5.92×10^3	4.44×10^3	5.33
D2_1588	70.9	zero	5.08×10^6	8.47×10^3	6.45×10^3	3.71
B3_1588	70.9	adverse	5.88×10^6	9.94×10^3	7.45×10^3	3.16
A8_1588	70.9	adverse $\cong 0$	1.08×10^7	2.41×10^4	1.82×10^4	1.30

The locations of the transducers considered in table 2 are shown in figure 3. The spectra of pressure fluctuations for the four transducers are shown in figure 8. The Corcos corrected spectra are shown in figure 9. The rolloff in the spectra at higher frequencies is evident and is consistent with the trends in r/δ^* as seen in table 2. The Strouhal number modification for this set of data is shown in figure 10. As was the case for the previously discussed set of data, the high frequency attenuation begins at a modified Strouhal number of 0.3. Scaling the amplitude by the factor $\left(r/\delta^*\right)^{1/2}$ does not produce consistent results in this case, as seen in figure 11. Further scaling of the amplitude by the factor r/δ^* (figure 12) produces slightly more consistent results. The largest amplitude variation between turbulence spectra in figure 11 is 4 dB, while in figure 12, the variation is 2 dB.

CONCLUSIONS AND RECOMMENDATIONS

The main conclusion of this report is that differences in Corcos corrected turbulent pressure fluctuation spectra, due to spatial resolution effects, can be resolved by multiplying the Strouhal number by the factor $\left(r/\delta^*\right)^{1/2}$. The amplitude also scales well with $\left(r/\delta^*\right)^{1/2}$ but is somewhat inconsistent.

The results presented in this report are from relatively large pressure transducers ($r/\delta^* > 1.0$). This work should be extended to measurements made with transducers having $r/\delta^* < 1.0$. If these results are consistent with those from smaller transducers, it may be possible to include the $\left(r/\delta^*\right)^{1/2}$ effects in the Corcos correction factors.

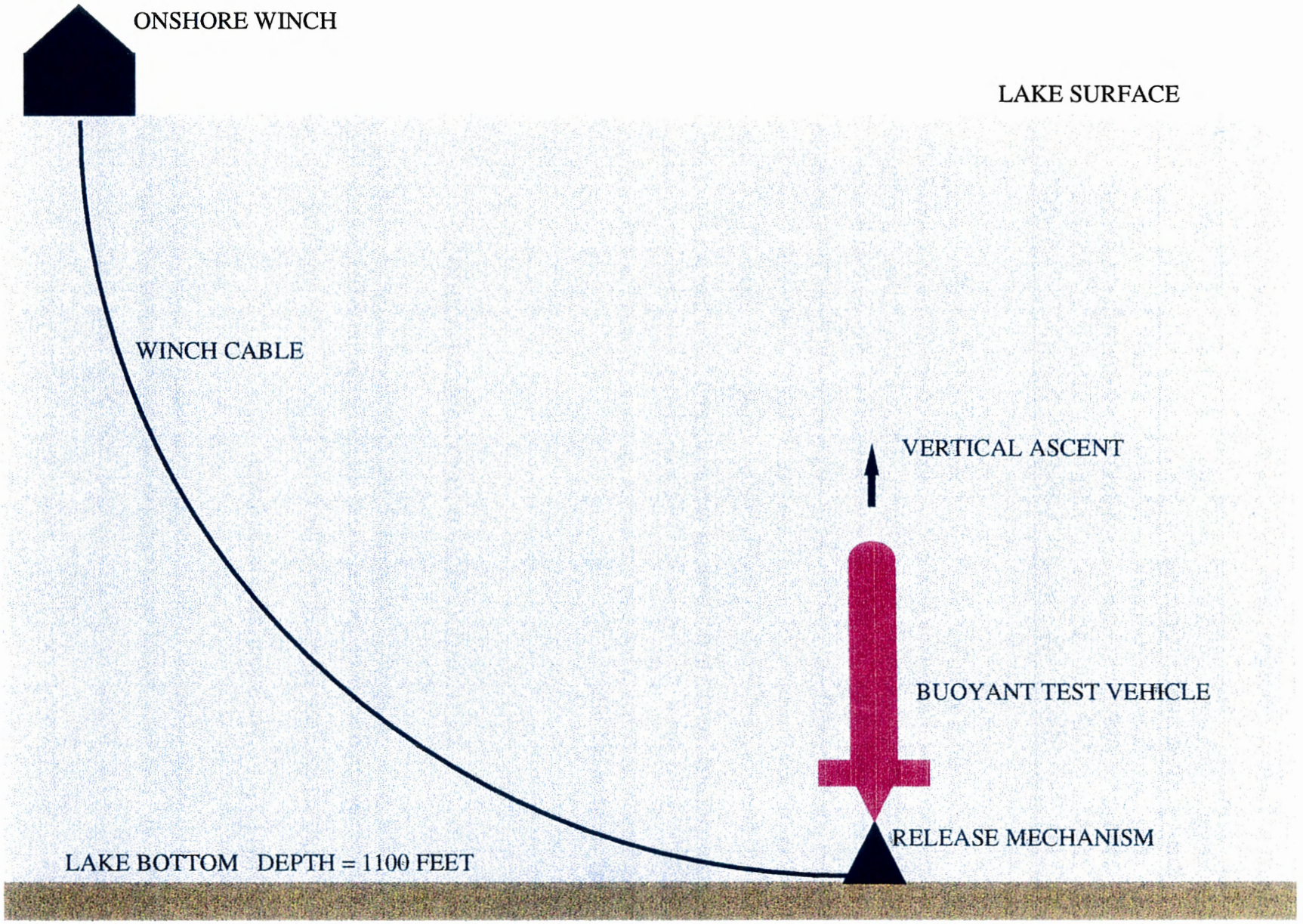

Figure 1: Experiment Setup

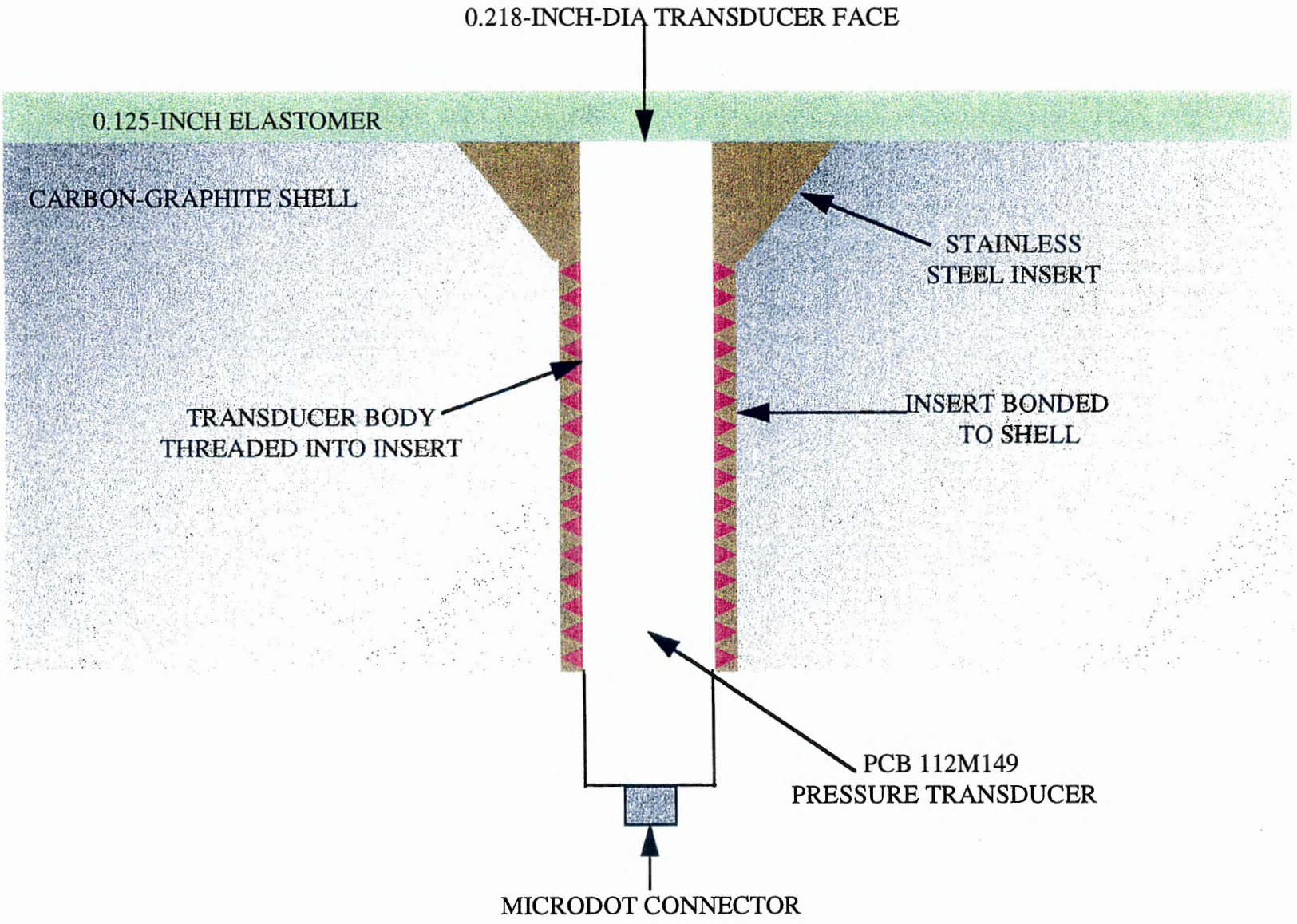

Figure 2: Pressure Transducer Mounting Technique in Carbon-Graphite Nose Shell

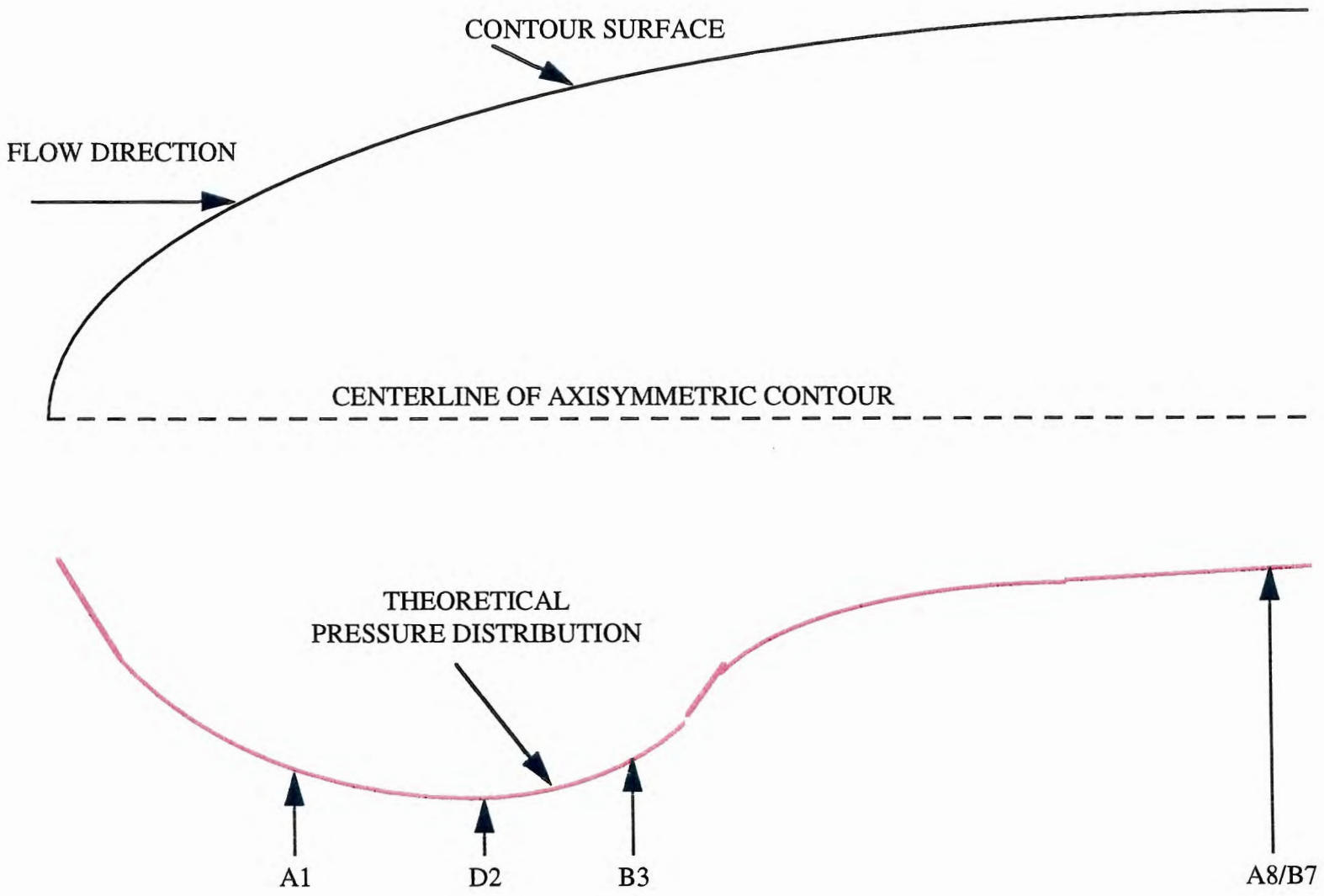

Figure 3: Nose Contour, Pressure Distribution, and Transducer Locations

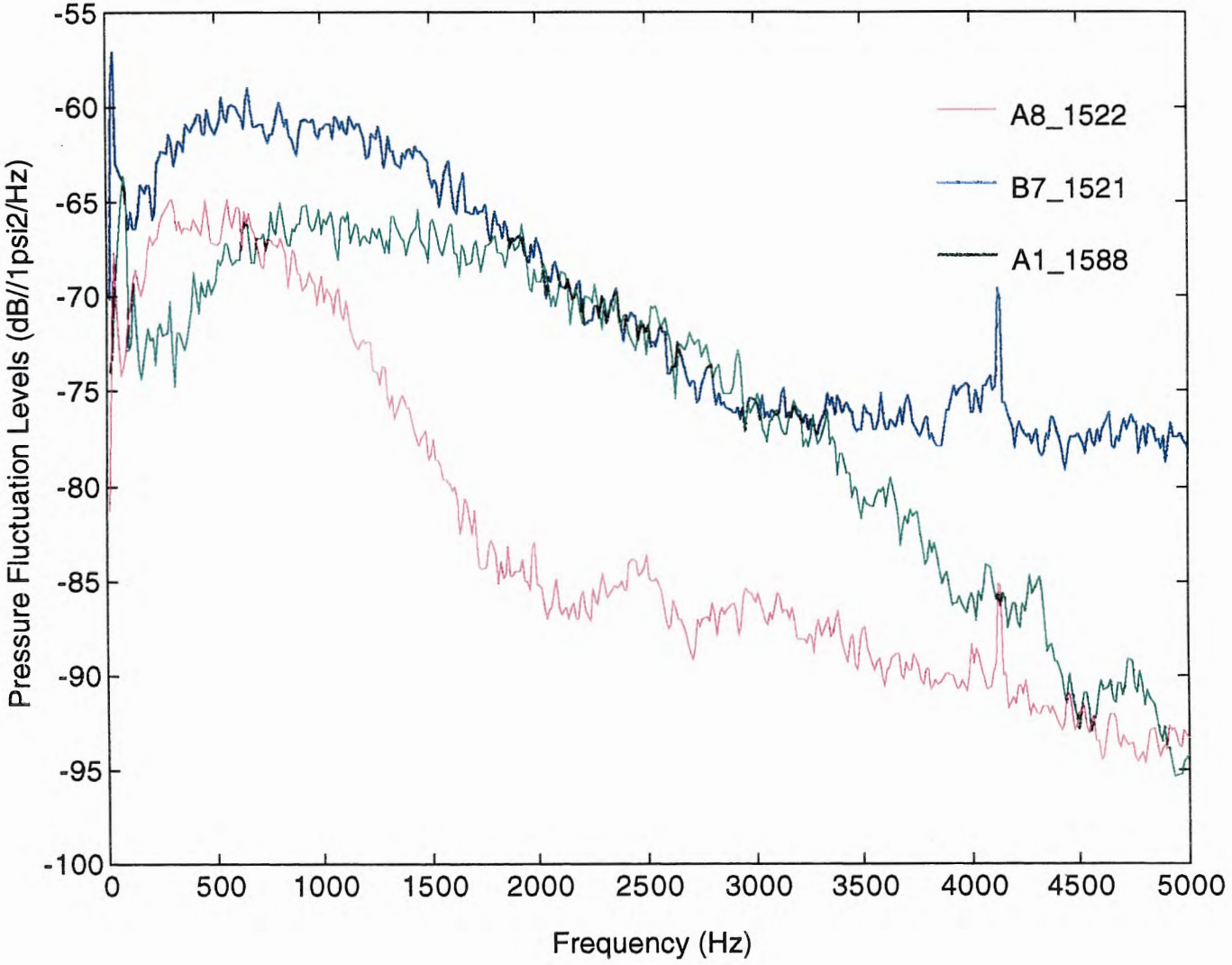

Figure 4: Dimensional Pressure Fluctuation Spectra (Case 1)

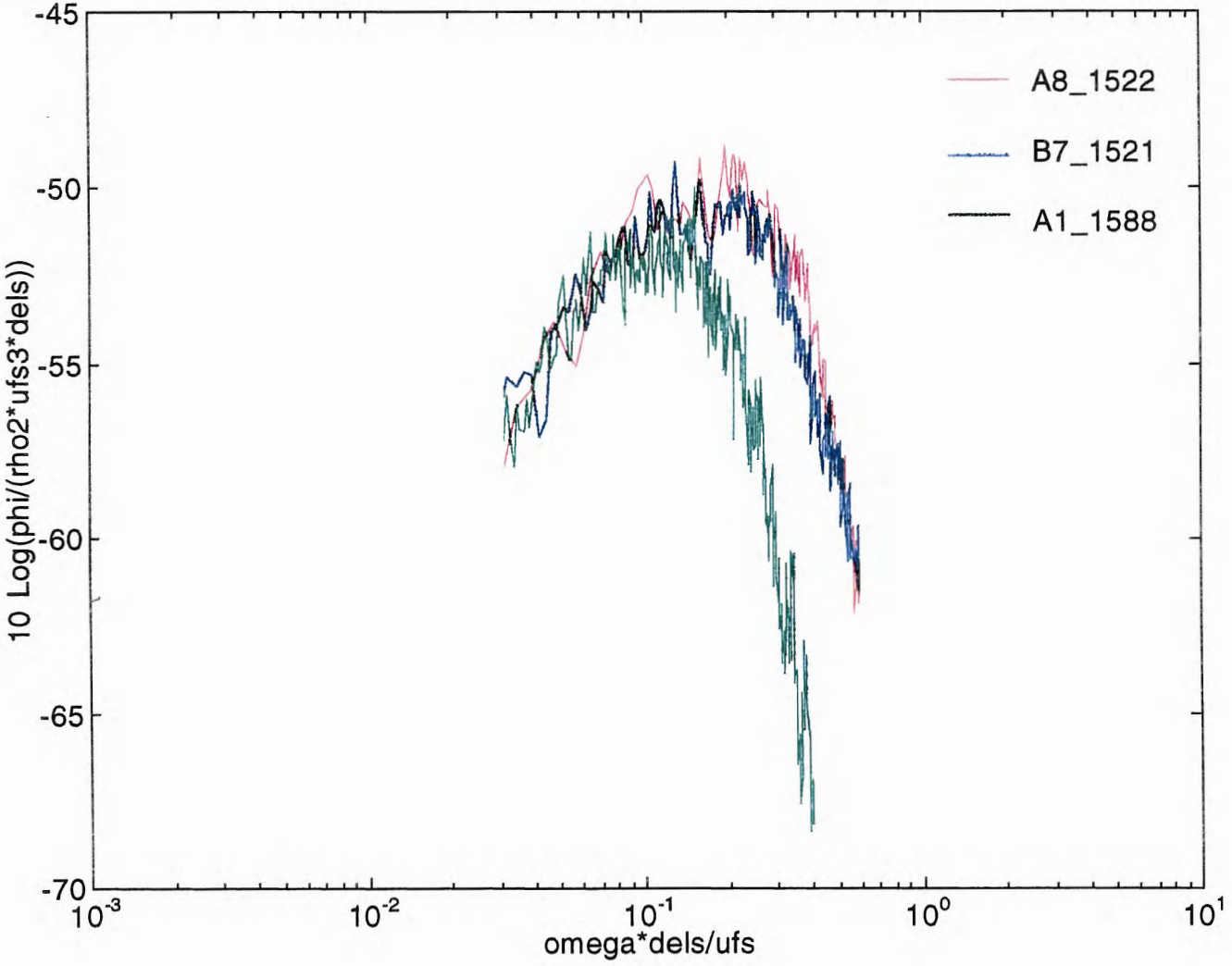

Figure 5: Corcos Corrected Spectra (Case 1)

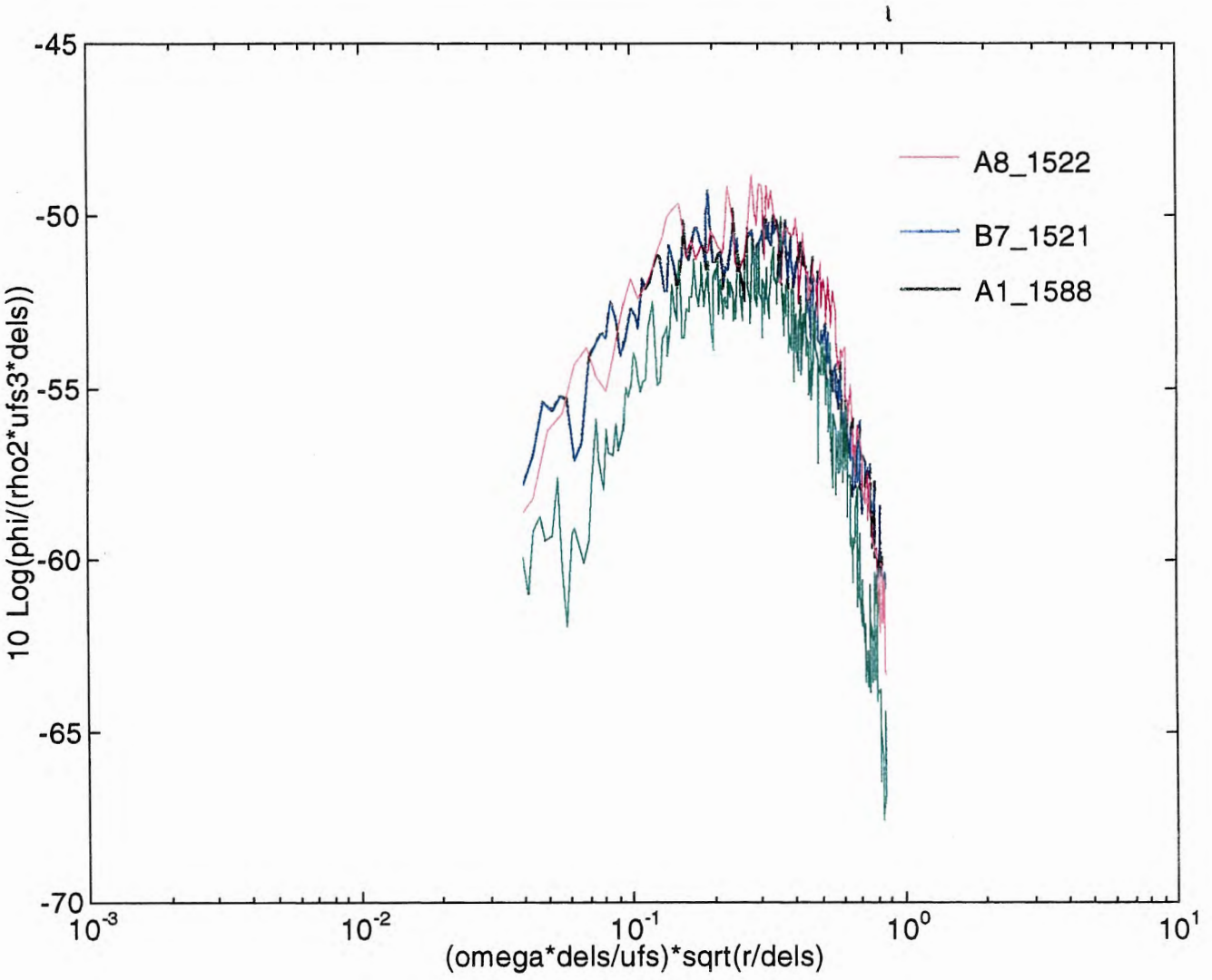

Figure 6: Corcos Corrected Spectra with $\left(r/\delta^*\right)^{1/2}$ Frequency Modification (Case 1)

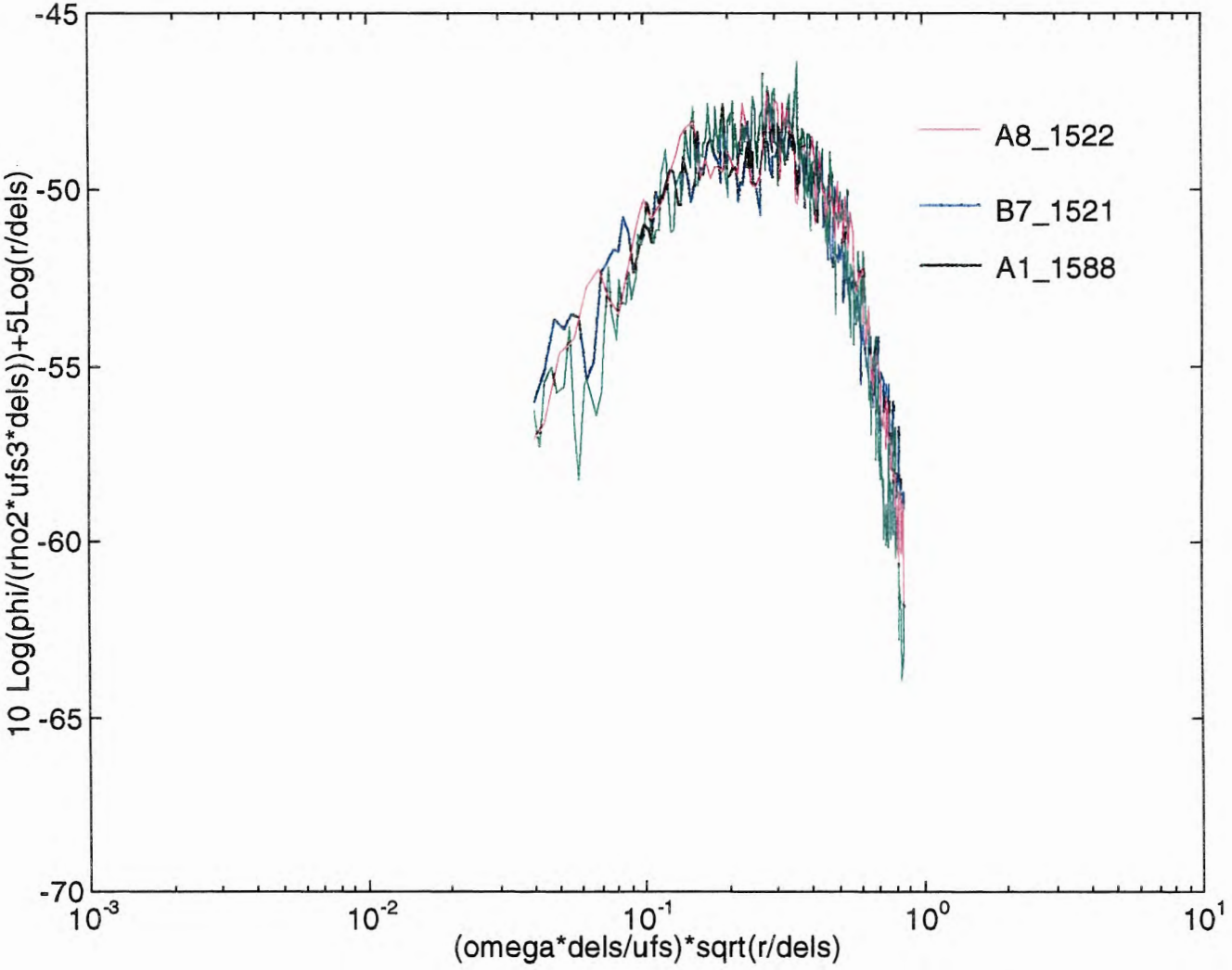

Figure 7: Corcos Corrected Spectra with $\left(r/\delta^*\right)^{1/2}$ Frequency and Amplitude Modifications (Case 1)

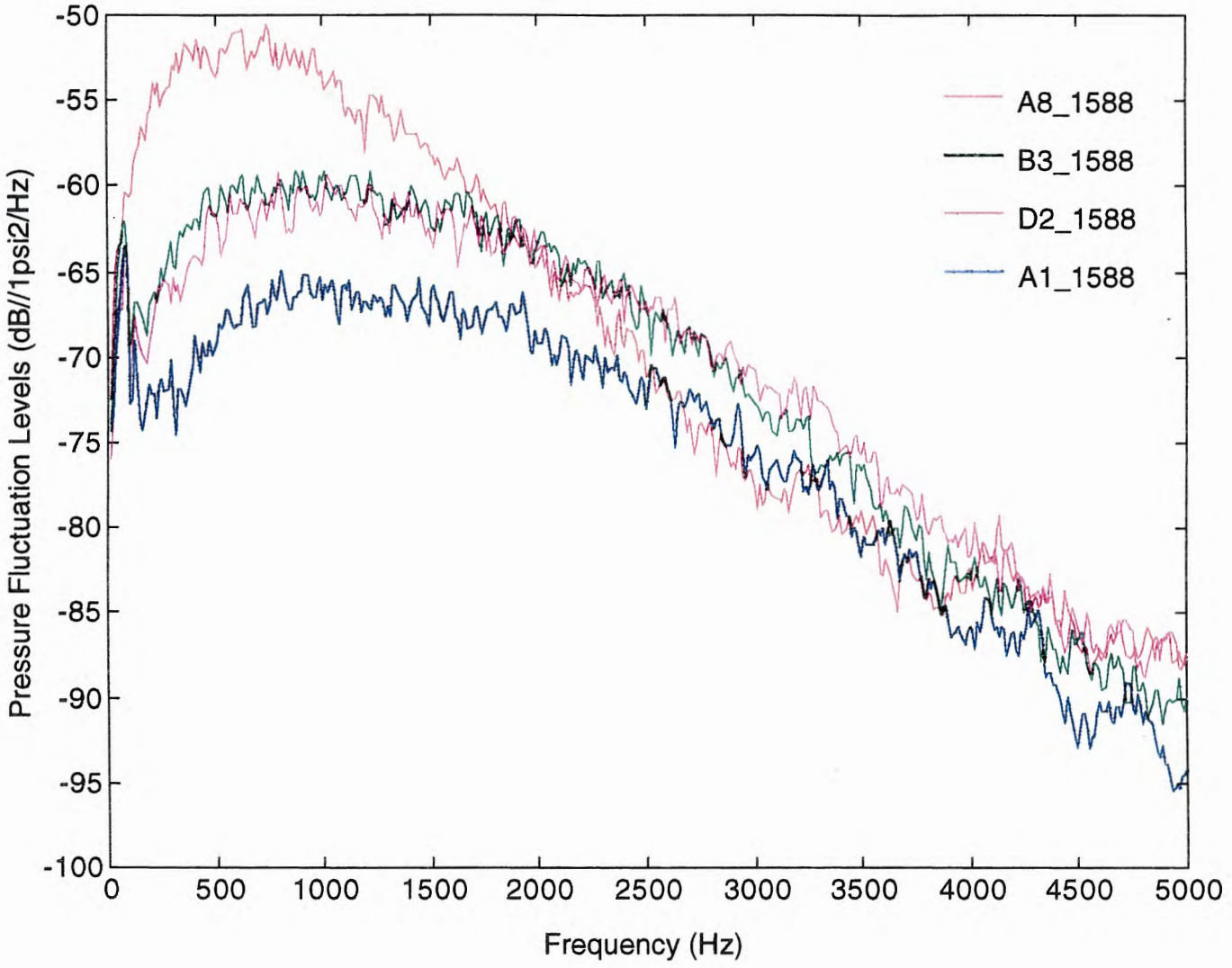

Figure 8: Dimensional Pressure Fluctuation Spectra (Case 2)

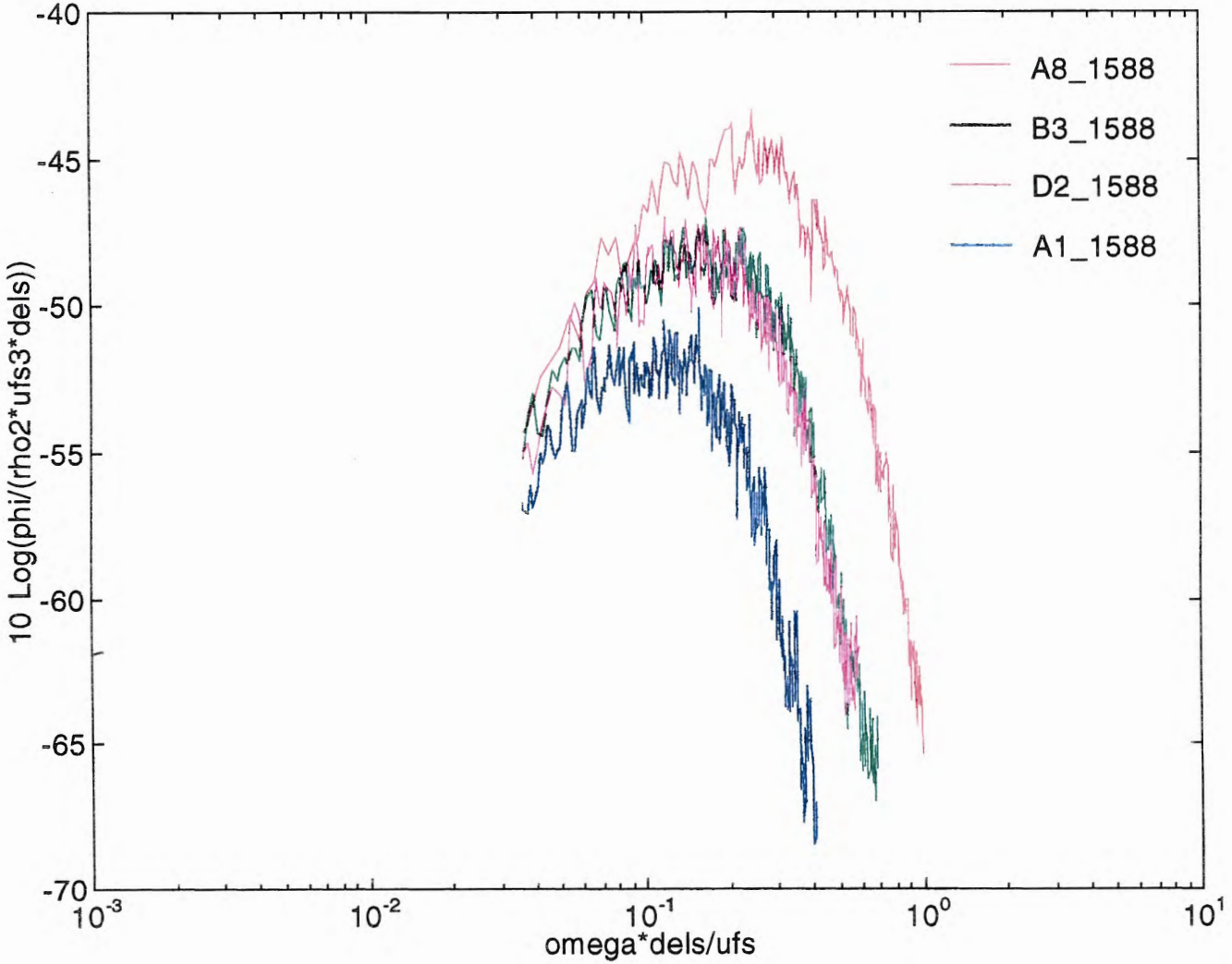

Figure 9: Corcos Corrected Spectra (Case 2)

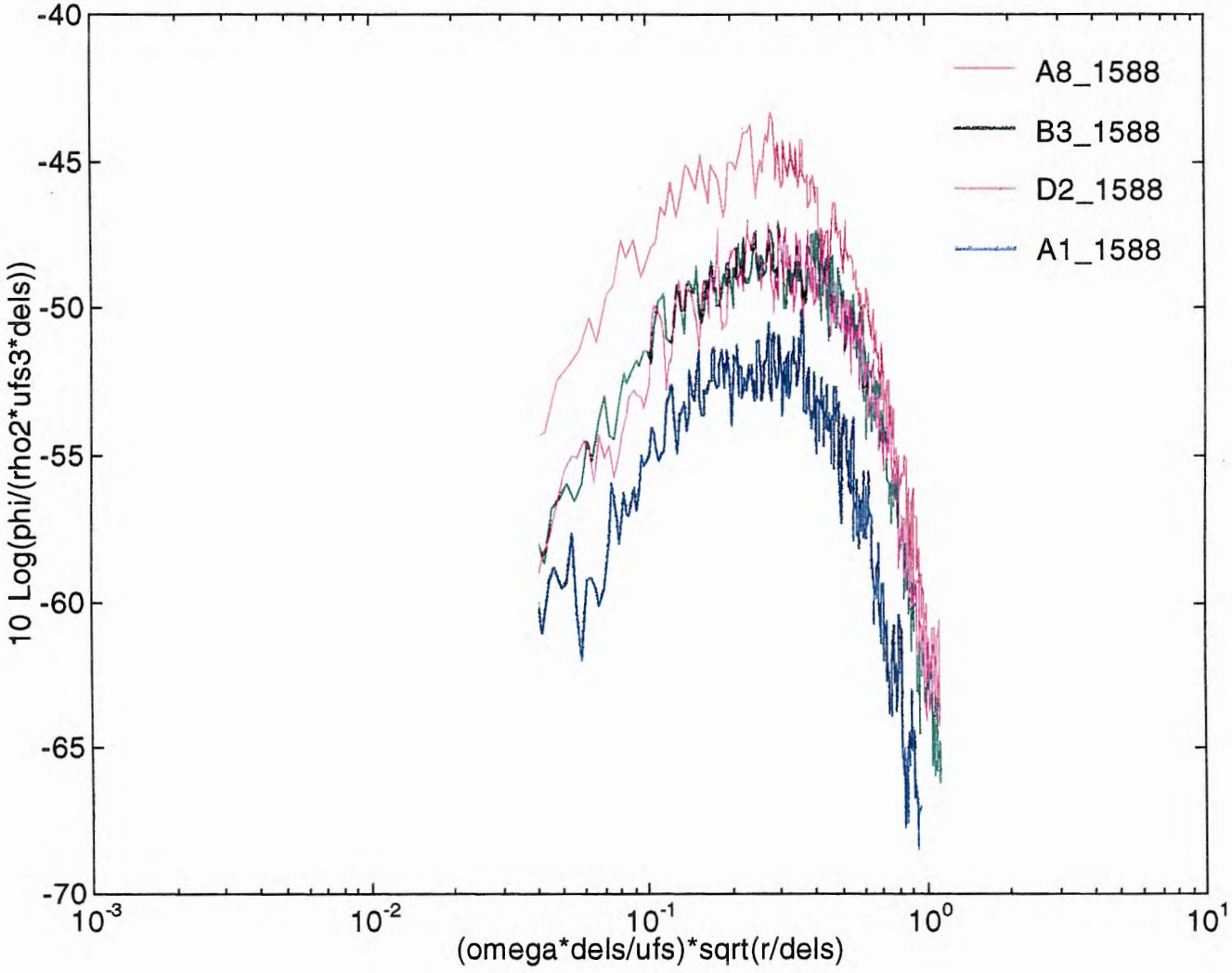

Figure 10: Corcos Corrected Spectra with $\left(r/\delta^*\right)^{1/2}$ Frequency Modification (Case 2)

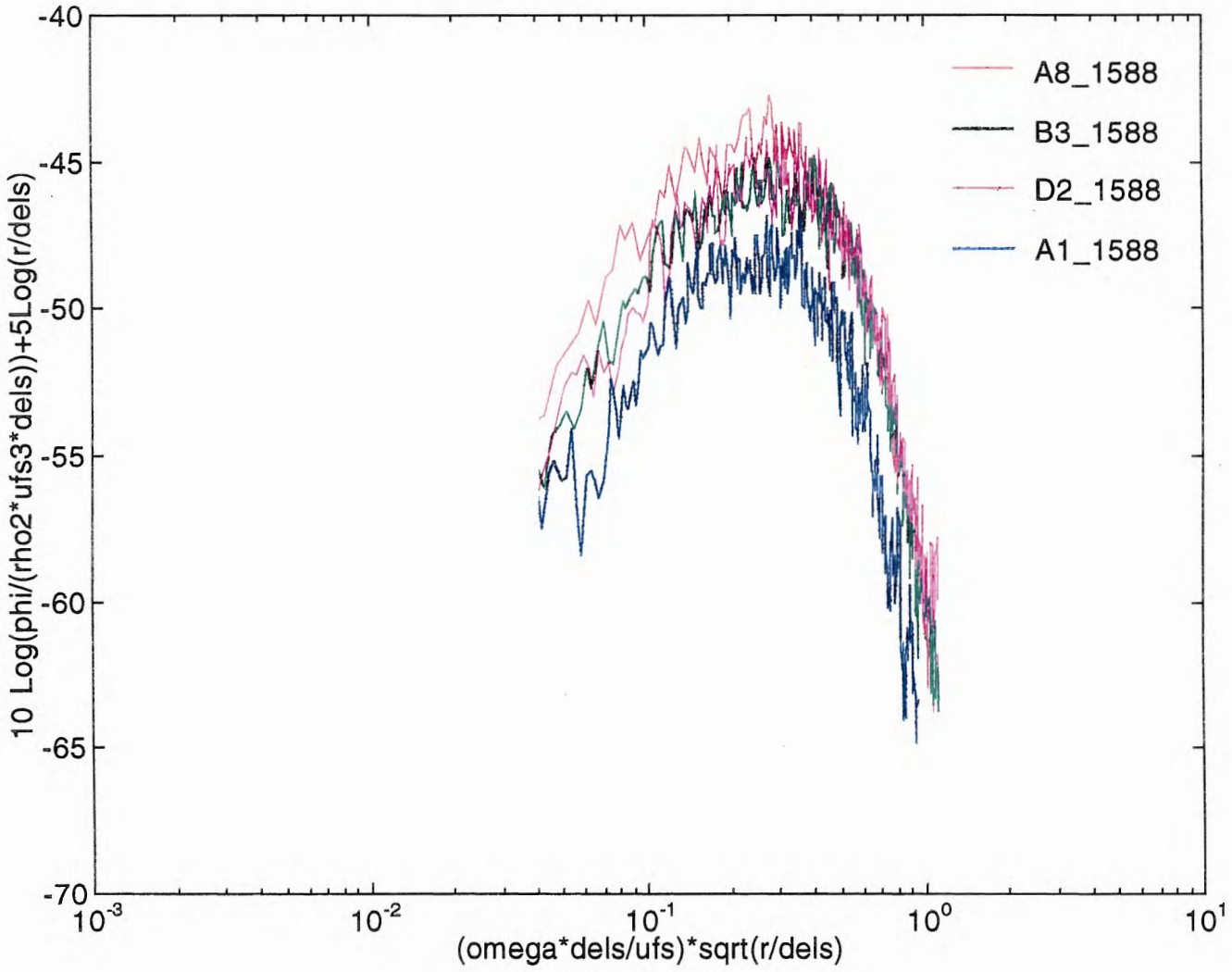

Figure 11: Corcos Corrected Spectra with $\left(r/\delta^*\right)^{1/2}$ Frequency and Amplitude Modifications (Case 2)

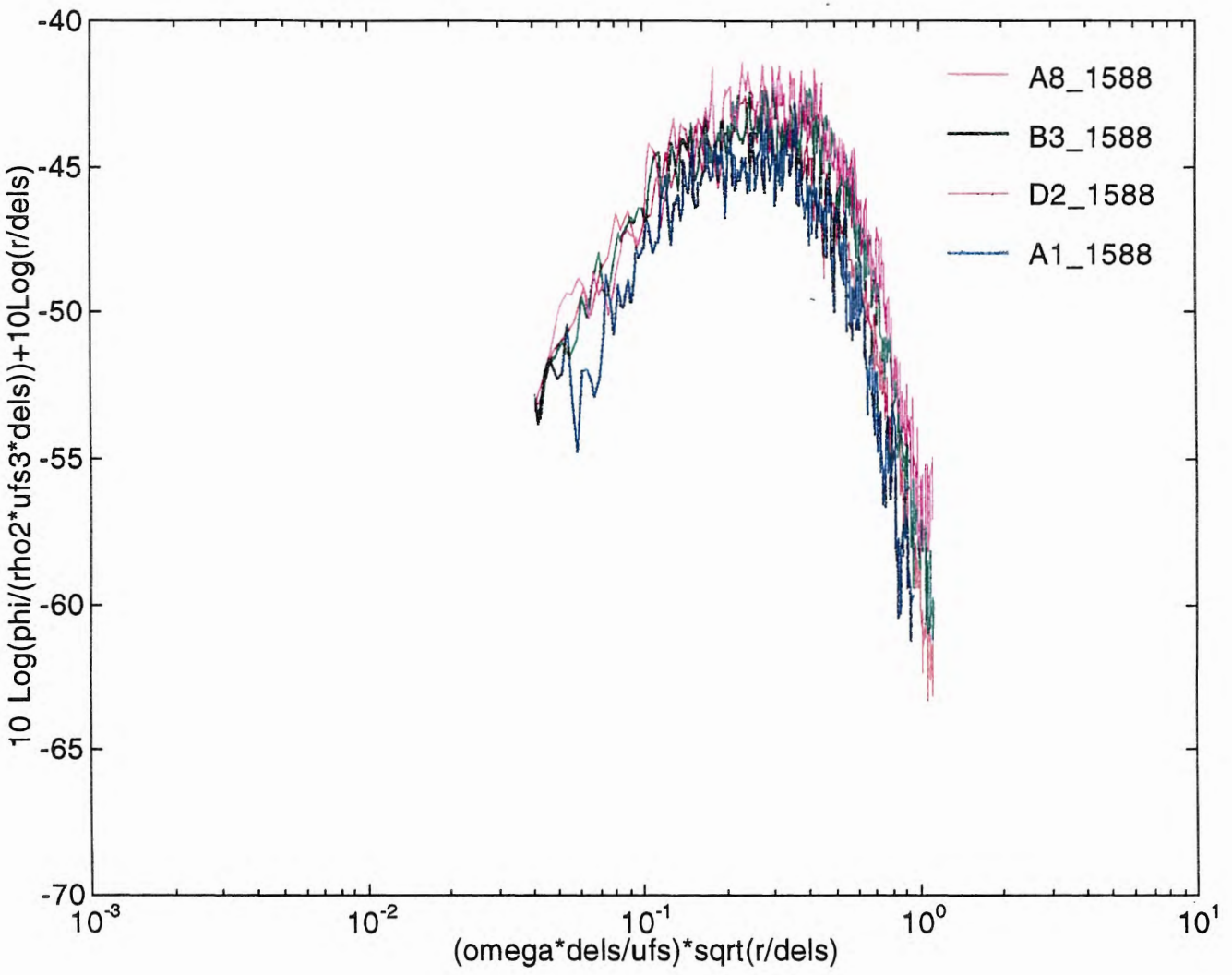

Figure 12: Corcos Corrected Spectra with $\left(r/\delta^*\right)^{1/2}$ Frequency and r/δ^* Amplitude Modifications (Case 2)

REFERENCES

1. Corcos, G.M., "Resolution of Pressure in Turbulence," J. Acoust. Soc. Amer., Vol 35, No. 2, pp 192-199, 1963.

2. Keith, W.L., Hurdis, D.A., and Abraham, B.M., "A Comparison of Turbulent Boundary Layer Wall-Pressure Spectra," J. Fluids Eng., Vol 114, pp 338-347, September 1992.

3. Galib, T.A., and Zadina, A., "Turbulent Pressure Fluctuation Measurements with Conventional Piezoelectric and Miniature Piezoresistive Transducers," NUSC TM 84-2045, 30 April 1984 (UNCLASSIFIED).

4. Galib, T.A., Katz, R., Ko, S., and Sandman, B., "Measurements of Turbulent Pressure Fluctuations using a Buoyant Vehicle Coated with a Thin Elastomer Layer," J. Acoust. Soc. Amer., Vol 96, No. 6, pp 3800-3803, December, 1994.

5. Gentry, A.E. and Wazzan, A.R., "The Transition Analysis Program System, Volume II," McDonnell-Douglas Report No. MDC J7255/02, June 1976 (UNCLASSIFIED).

DISTRIBUTION LIST

External

NSWC Code 27 (D. Dozier)
NSWC Code 725 (L. Grega)
Noesis, Inc. (G. Letiecq)
ARL/PSU (G. Lauchle, T. Brungart)

Internal

Codes: 01 (B. Sandman)
019 (G. McNamara)
10
2002 (H. Schloemer)
213 (R. Elswick)
2133 (D. Glenning, S. Ko)
2141 (B. Abraham, D. Hurdis, W. Keith)
31
3113 (R. Katz)
5441 (2)
70
80
81
811
8112 (R. Tompkins, D. Quadrini, T. Galib (10))
812
82
8233 (P. Bandyopadhyay, J. Castano)
83

Total: 40